Non-Fermi Liquid Behavior and Continuously Tunable Resistivity Exponents in the Anderson-Hubbard Model at Finite Temperature

Niravkumar D. Patel, Anamitra Mukherjee, Nitin Kaushal, Adriana Moreo, and Elbio Dagotto

Phys. Rev. Lett. **119**, 086601 — Published 24 August 2017

DOI: 10.1103/PhysRevLett.119.086601

Non Fermi liquid behavior and continuously tunable resistivity exponents in the Anderson-Hubbard model at finite temperature

Niravkumar D. Patel[1], Anamitra Mukherjee[2], Nitin Kaushal[1], Adriana Moreo[1,3], and Elbio Dagotto[1,3]
[1]*Department of Physics and Astronomy, The University of Tennessee, Knoxville, Tennessee 37996, USA*
[2]*School of Physical Sciences, National Institute of Science Education and Research, HBNI, Jatni 752050, India and*
[3]*Materials Science and Technology Division, Oak Ridge National Laboratory, Oak Ridge, Tennessee 37831, USA*
(Dated: July 26, 2017)

We employ a recently developed computational many-body technique to study for the first time the half-filled Anderson-Hubbard model at finite temperature and arbitrary correlation (U) and disorder (V) strengths. Interestingly, the narrow zero temperature metallic range induced by disorder from the Mott insulator expands with increasing temperature in a manner resembling a quantum critical point. Our study of the resistivity temperature scaling T^α for this metal reveals non Fermi liquid characteristics. Moreover, a continuous dependence of α on U and V from linear to nearly quadratic was observed. We argue that these exotic results arise from a systematic change with U and V of the "effective" disorder, a combination of quenched disorder and intrinsic localized spins.

A hallmark of a conventional Fermi liquid (FL) in good metals is the T^2 scaling of the resistivity (ρ) with temperature T. However, deviations from this behavior have been reported in several correlated electronic materials such as heavy fermions [1–4], rare earth nickelates [5], layered dichalcogenides [6], and cuprates [7–9]. Various ideas for explaining non Fermi liquid (NFL) states have been proposed. For instance, a $T = 0$ quantum critical point (QCP) could induce the linear $\rho \sim T$ scaling in the cuprates [9–11]. In the NFL observed in the two-dimensional electron gas (2DEG) [12–14], charge or spin glassy metallic states could provide an alternative [15–18]. In spite of these important efforts, the understanding of NFLs in correlated systems still eludes theorists. Moreover, in heavy fermion experiments a puzzling continuous variation of the ρ vs. T scaling exponent α between 1 and 1.6 was found [1–4]. Considering that the microscopic physics of the several NFL material families are quite different, it is a challenge to find a global understanding of NFL states in correlated systems. In particular, we need to identify concrete model Hamiltonian systems that not only support NFL states but also, within a single framework, capture various NFL systematics observed across different material families.

To address these issues, here we study the temperature characteristics of the unconventional metal known to develop at $T = 0$ from the *competition* between strong electron interactions and disorder in the half-filled Anderson-Hubbard model on a square lattice. In the clean limit, the ground state is a Mott insulator (MI) and correlated metals arising from doping MI's [19] violate the $\rho \sim T^2$ scaling. In the other limit where quenched disorder dominates, single particle states are localized in two dimensions and these disorder-induced Anderson insulators often display variable range hopping behavior [20].

The surprising $T = 0$ intermediate metallic state that results from the combination of correlations and disorder has been studied theoretically using statistical Dynamical Mean Field Theory (DMFT) [21–26], Quantum Monte Carlo [27–29], Exact Diagonalization [30], Hartree-Fock [31] and typical medium theory [32] and its cluster extensions [33] that allows direct identification of Anderson localized states.

Experimental results [6, 34–37] are compatible with the zero temperature calculations. However, the finite temperature understanding of this exotic metal and its scaling is limited and several questions remain. How does a metal that arises from competing Mott and Anderson insulators behave at finite temperatures? What temperature scaling does the resistivity of the ensuing metal display? Is there a dependence of the exponent α on disorder and interaction strengths that can be tuned? Are spin or charge cluster states [18] responsible for such scaling behavior? Answers to these open questions are of relevance for experiments and theory alike.

In this publication, we study the half-filled Anderson-Hubbard model at finite temperature using the recently developed Mean Field-Monte Carlo (MF-MC) technique. This approach properly incorporates thermal fluctuations in a mean field theory [38]. Details and benchmarks are in *Supplementary Material Sec. I* [39]. Using MF-MC, here we establish the disorder-interaction-temperature ($V - U - T$) phase diagram. In particular, we observed a disorder-induced continuous evolution from the Mott to the Anderson insulators with a strange metal in between. Our temperature analysis of this region unveils an intriguing quasi QCP behavior, with a narrow metallic region increasing in width with increasing temperature resembling a quantum phase transition. Through optical conductivity and resistivity calculations, we uncover a striking behavior: by changing U and V, α can be tuned (akin to heavy fermions) from linear $\alpha = 1$, as in cuprates, to near quadratic. Then disorder and interactions can be used to modify the scaling $\rho \sim T^\alpha$.

The model is:

$$H = -t \sum_{\langle i,j \rangle\ \sigma} c^\dagger_{i,\sigma} c_{j,\sigma} + \sum_i U n_{i\uparrow} n_{i\downarrow} + \sum_i (V_i - \mu)(n_{i\uparrow} + n_{i\downarrow}),$$

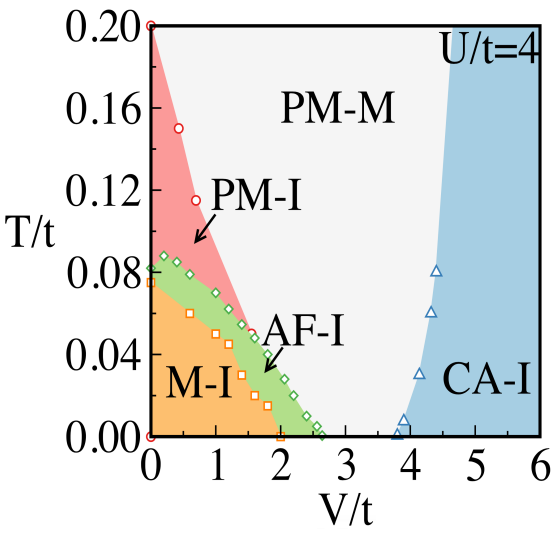

FIG. 1. (color online) Temperature (T) vs. disorder (V) phase diagram at half filling for $U/t = 4.0$ obtained using a 32^2 square lattice. The zero temperature antiferromagnetic (AFM) Mott insulator (M-I) to gapless AFM insulator (AF-I) at $V \sim 2t$, and the subsequent transition to the paramagnetic metal (PM-M) at $V \sim 3t$, are both continuous within our accuracy. For $V > 3.8t$ at $T = 0$, we observe a disorder-induced correlated Anderson insulator (CA-I). Finally for $T/t \in [0.08, 0.2]$ and small V/t, pink region, we find a gapless PM insulator (PM-I). Details are in the text.

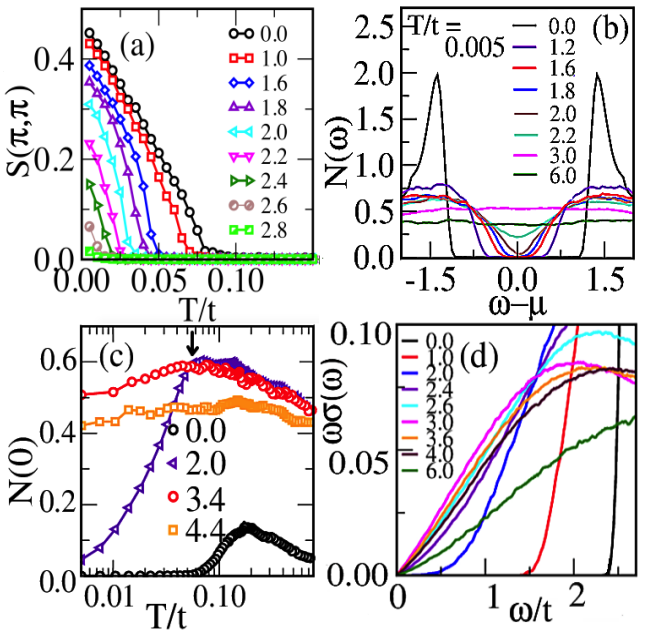

FIG. 2. (color online) Examples of MF-MC data at $U/t = 4$ used to construct the phase diagram Fig. 1. (a) Static magnetic structure factor at $q = (\pi, \pi)$. Values of V/t are in the column. (b) Low-T density-of-states (DOS) $N(\omega)$ at various disorder strengths. (c) DOS $\omega = 0$ weight at the four V/t's indicated vs. T/t. Arrow indicates the maximum of $N(0)$ for $V/t = 3.4$. (d) ω times the optical conductivity $\sigma(\omega)$, at $T/t = 0.005$, for the several V/t's indicated.

where the first term is the kinetic energy and the second the standard Hubbard repulsion. $c_{i\sigma}$ ($c^\dagger_{i\sigma}$) annihilates (creates) an electron at site i with spin σ. The number operator is $n_{i\sigma} = c^\dagger_{i\sigma} c_{i\sigma}$. The disorder V_i at each site is chosen randomly in the interval $[-V, V]$ with uniform probability. The chemical potential μ is adjusted to achieve half filling globally. In MF-MC, we first Hubbard-Stratonovich decouple the interaction term, by introducing vector $\mathbf{m}_i$ and scalar ϕ_i auxiliary fields at every site. The former couples to spin and latter to charge. Dropping the time dependence of the auxiliary fields (Aux. F.) a model with "spin fermion" characteristics arises. The Aux. F. are treated by classical MC that admits thermal fluctuations, and the fermionic sector is solved using Exact Diagonalization. Details of the considerable numerical effort involved are discussed in *Supplementary Material Sec I.*

1. Phase diagram. Consider the phase diagram shown in Fig. 1 at the representative value $U/t = 4$. Various indicators, such as the (π, π) static magnetic structure factor [40], density of states (DOS), and optical conductivity $\sigma(\omega)$ were used (Fig. 2). At $T/t = 0.005$ the antiferromagnetic (AFM) order is progressively reduced increasing V/t as shown in Fig. 2 (a), and for $V \geq 2.6t$ the signal becomes negligible. At $V = 0$, the magnetic order starts at $T/t = 0.10$ upon cooling but the system remains insulating above this temperature, as expected, and a paramagnetic insulator (PM-I), is deduced based on the optical conductivity behavior discussed below. Increasing V/t, T_N initially slightly increases and then reduces with increasing disorder [41]. The metal insulator boundary decreases roughly linearly with V/t, collapsing to zero at $V/t = 2.6$. Panel (b) shows the low-T DOS, $N(\omega)$, for various disorder strengths. We find that the clean-limit Mott gap evolves into a pseudogap gap at $V/t \sim 2$. This pseudogap persists up to $V/t = 2.8$ and flattens out for larger V/t, with the weight around $\omega = 0$ decreasing gradually with disorder as the DOS spreads over a larger energy range due to increasing scattering. Thus, the AF-I, PM-M and CA-I phases in Fig. 1 are gapless.

Figure 2 (d) shows $\omega\sigma(\omega)$ at $T = 0$ for different disorder values covering the Mott-Insulator, the strange metal, and the large disorder (CA-I) phases. For $V/t \leq 2.0$, $\sigma(\omega)$ is clearly gapped. In the narrow range $2.0 < V/t < 2.6$, $\omega\sigma(\omega)$ tends to zero as $\omega \to 0$ in a non-linear manner. For $2.6 \leq V/t \leq 3.8$, $\omega\sigma(\omega) \to 0$ linearly i.e. $\sigma(\omega)$ is constant at small ω indicating a metal. For the CA-I, variable range hopping is expected to provide a $\omega^3 ln^3(I/\omega)$ behavior [20], where I is a typical energy scale depending on the localization length. Fig. 3 in *Supplementary Material Sec II* that discusses our optical conductivity results [42], show that the same be-

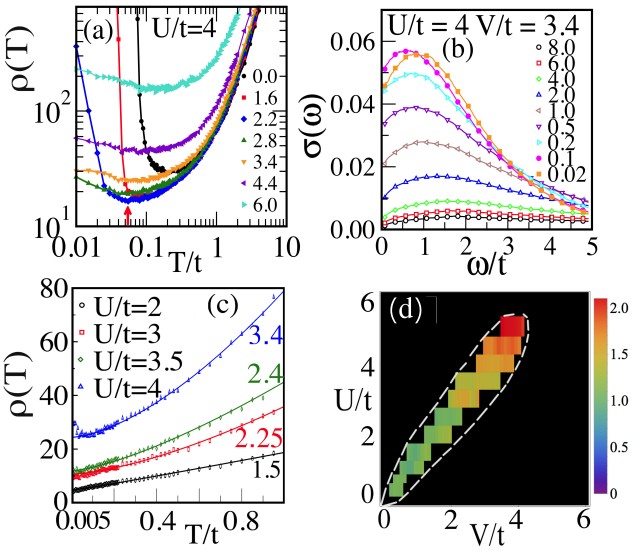

FIG. 3. (color online) (a) ρ ($\pi e^2/\hbar a_0$ units) vs. T/t at $U/t = 4$ and the various V/t's in the column (a_0 is the lattice spacing, set to 1). The red arrow at the bottom shows ρ_{min} for $V/t = 3.4$. (b) Optical conductivity at $U/t = 4$ and $V/t = 3.4$ displaying non-Drude behavior, at the T/t's in the column. (c) $\rho(T)$ at special values of U/t and V/t such that the state is metallic almost in all the T/t range shown. Solid lines are fits to $\rho(0) + AT^{\alpha}$. For $U/t = 2,\ 3,\ 3.5$, and 4.0, and the V/t values indicated (color, right), α is 1.02, 1.35, 1.39, and 1.68, respectively. (d) The metallic window in the $U - V$ plane at low temperature $T/t = 0.005$ is shown by the colored region (the dashed line just guides the eye). The black region denotes insulator. The color of the metallic region depicts the value of α arising from the T^{α} scaling of $\rho(T)$.

havior holds across the finite T insulator to metal transitions as well. This numerical criterion, certain subtleties and consistency with inverse participation ratio (IPR) are also discussed in *Supplementary Material Sec II*. We have used this criterion to determine all metal insulator boundaries in Fig. 1. Our $T = 0$ phase boundaries are in excellent agreement with earlier literature [31, 43] and our metal and insulating phases *both* at zero and finite temperatures are robust against finite size scaling (*Supplementary Material*, Fig. 4). We now shift the focus to our main contributions at finite T.

2. Non Fermi liquid metal. The resistivity extracted from $1/\sigma(\omega)$ at small ω (see supplementary) is in Fig. 3 (a) for $U/t = 4$. There are several important features: (i) $d\rho/dT$ becomes positive at large T for all values of V/t; (ii) For the PM-I regime at $V/t = 0$ and 1.6, $d\rho/dT$ becomes negative with eventual divergence at the critical AFM temperature. Further, based on optical conductivity behavior (*Supplementary material Sec.II*) and finite DOS weight at Fermi energy ($N(0)$) beyond $T/t = 0.08$ for $V = 0$ in Fig. 2 (c), the PM-I is a gapless insulator. For the metallic ($V/t = 2.8$ and 3.4) and the CA-I ($V/t = 4.4$ and 6.6) phases, $\rho(T)$ saturates at the lowest T's investigated [44]. (iii) There are resistivity minima at finite T which coincide with the corresponding location of the peaks in $N(0)$ in Fig. 2 (c) at, *e.g.*, $V/t = 3.4$. The NFL nature of the disorder-induced metallic state can be inferred from panel (b) which shows that $\sigma(\omega)$ has a non-Drude form with a peak at finite frequency. This peak is further pushed to higher frequency with increasing T, except at very low T when the peak converges to $\omega/t \sim 1$.

Both $\rho(T)$ here, and specific heat (C_v) in *Supplementary Material* Fig. 5, show low T deviations from FL behavior consistent with literature on disorder induced NFLs [18], justifying our "NFL metal" nomenclature.

Consider now the ρ vs. T behavior for the NFL state. In the metallic regime ($V/t = 3.4$), the resistivity minimum occurs at $T/t \sim 0.1$. From Fig. 2 (c) at $V/t = 3.4$, the location of ρ_{min} coincides with the peak in $N(0)$ at $T/t \sim 0.055$. This non-monotonic dependence of $N(0)$ on T agrees with DQMC studies of the Hubbard model [45] for $V = 0$.

The initial increase of $N(0)$ is due to thermally induced fluctuations that enhance the DOS weight at $\omega = 0$. At high T, the scattering of fermions from the Aux. F.'s suppress $N(0)$, and this non-monotonicity is reflected in the metallic-like thermal behavior of $\rho(T)$. In summary, at low T the initial increase of the DOS at the Fermi level forces $d\rho/dT$ to be negative, while at high T this DOS is suppressed again because of the localized spins and $d\rho/dT$ changes sign.

3. Scaling of resistivity. In Fig. 3 (c) we show $\rho(T)$ for combinations of U/t and V/t where the system is a metal over a wide temperature range. The full map of the low temperature metallic region in the $U/t - V/t$ plane is in Fig. 3 (d). The resistivity data is fitted to $\rho(0) + AT^{\alpha}$ for each case to extract α [46]. For small/intermediate values of ($U/t,\ V/t$) (open circles), $\rho(T)$ grows linearly with T in the range analyzed. For larger U/t (and corresponding V/t) α increases from $\sim$1.0 to 1.7 for $U/t = 2,\ V/t = 3.4$. As shown in Fig. 3 (d), the metallic window at $T/t = 0.005$ occurs roughly around the line $U \sim 1.25V$ [47]. The dashed line guides the eye and it envelops the metallic region. The metallic-regime color scale indicates the value of α in the temperature fit of $\rho(T)$. For up to $U/t = 2.5$, $\alpha \sim 1$ growing slowly with U/t (the smallest values checked are $U/t = 0.5,\ V/t = 0.5$). For larger $U/t, V/t > 2.5$, α grows reaching a maximum value close to 2 for $U/t = 5$ [48]. This $\alpha \sim 2$ does not imply a FL but we believe it is just one of the possible transport exponents that occurs in our system in its slow evolution. For even larger U/t, within our precision the metallic region closes. Finally, old DQMC calculations [29], show hints of such scaling, exhibiting robustness of our results in presence of quantum fluctuations.

4. Discussion. To better understand the combined effect of disorder and interaction in the metallic phase, in Fig. 4 (a) we show the variance of the local density $\{n_i\}$, defined as $\delta n(U,\ V,\ T) = \langle\sqrt{\langle n\rangle^2 - \langle n^2\rangle}\rangle$. The outer an-

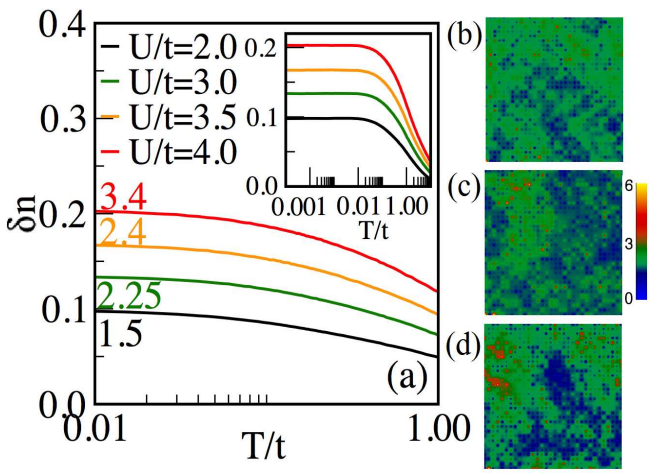

FIG. 4. (color online) Fluctuations in the charge density vs. T at various U/t's and V/t's (color), in the metallic regime. Inset contains the same data up to $T/t = 10$. (b,c,d) show real-space maps of $|\psi(r)|^2$ at the Fermi energy using 32^2 systems at $T/t = 0.2$ and coupling strengths $(U,\ V) = (2.0t,\ 1.5t)$, $(3.0t,\ 2.25t)$ and $(4.0t,\ 3.4t)$, respectively. Color scale indicates the range of values for $|\psi(r)|^2$ in 10^{-3} units. Data in (a) to (d) are averaged over 10 MC samples for a fixed disorder realization.

gular brackets imply averaging over MC samples at fixed T, while the inner ones are the quantum average within a single MC sample. There are two sources of disorder that control the variance of $\delta n(U,\ V,\ T)$. First is the static disorder (V) with variance δV and the second are the Aux. F.'s. These Aux. F.'s directly couple to the fermions and indirectly to the disorder through the local fermion occupations (Sec. I of the *Supplementary Material*). Then, the Aux. F. also provide an inhomogeneous background that at low temperatures follows the presence of intrinsic static disorder. But at temperatures where $k_BT \geq \delta V$, the intrinsic disorder (V) is unimportant and the Aux. F. configurations become homogeneous in average. Thus, $\delta n(U,\ V,\ T)$ remains non zero at low T while it tends to zero at large T, on MC sample averaging. This behavior is observed in the inset of Fig. 4 (a). In the main panel we show the same data between $T/t = 0.01$ and 1. We find a systematic increase in $\delta n(U,\ V,\ T)$ with increasing U/t and V/t. This variance manifests as real-space charge clusters as shown in Fig. 4 (b) to (d) that contains maps of $|\psi(r)|^2$ at fixed T, MC sample averaged, for states at the Fermi energy. With increasing U/t and V/t, the charge clustering and the charge fluctuations magnitude increase systematically following the increase in $\delta n(U,\ V,\ T)$. This provides a controlled enhancement in spatially inhomogeneous background from which the fermions scatter [49].

It is known that fermions coupled to classical variables such as disorder [50], adiabatic phonons [51] etc. can exhibit charge clustering, metallic glasses, and NFL behavior. Moreover, disorder-induced rare fluctuations (of charge/spin) similar to the results in Figs. 4 (b) to (d) are known to stabilize electronic Griffith's phases and NFL behavior [52, 53] with tunable critical exponents [54].

In our case, not only the quenched disorder but also the Aux. F. fluctuations play the role of the classical scatterer that give rise to NFL scaling. Such charge clusters and NFL behavior has been experimentally observed in the 2DEG near a $T = 0$ quantum critical point [12–14]. Here, within MF-MC, we have found such a "charge cluster metal" in the half-filled Anderson Hubbard model and also observed that their deviation from FL theory can be tuned. This tunability allows us to show that, in a single model Hamiltonian, the resistivity scaling with T can vary between linear to near quadratic, features observed in real NFLs like cuprates and heavy fermions. Our results thus represent progress towards identifying a single model system with NFL behavior transcending many material families.

Acknowledgments. A. Mukherjee acknowledges useful discussions with P. Majumdar, P. Chakraborty, and H. R. Krishnamurthy. N.P. and N.K. were supported by the National Science Foundation, under Grant No. DMR-1404375. E.D. and A. Moreo were supported by the U.S. Department of Energy, Office of Basic Energy Sciences, Materials Sciences and Engineering Division.

[1] P. Gegenwart *et al.*, Phys. Rev. Lett. **81**, 1501 (1998).
[2] O. Trovarelli *et al.*, Phys. Rev. Lett. **85**, 626 (2000).
[3] S. R. Julian *et al.*, J. Phys.: Condens. Matter **8**, 9675 (1996).
[4] P. Coleman, C. Pepin, Q. Si, and R. Ramazashvili, J. Phys.: Condens. Matter **13**, R723 (2001).
[5] R. Jaramillo, S. D. Ha, D. M. Silevitch, and S. Ramanathan, Nature Physics **10**, 304 (2014).
[6] E. Lahoud, O. N. Meetei, K. B. Chaska, A. Kanigel, and N. Trivedi, Phys. Rev. Lett. **112**, 206402 (2014).
[7] A. Damascelli, Z. Hussain, and Z.-X. Shen, Rev. Mod. Phys. **75**, 473 (2003).
[8] N. E. Hussey, M. Abdel-Jawad, A. Carrington, A. P. Mackenzie, and L. Balicas, Nature **425**, 814 (2003).
[9] B. Keimer, S. A. Kivelson, M. R. Norman, S. Uchida, and J. Zaanen, Nature **518**, 179 (2015).
[10] P. Anderson, Nature Physics **2**, 626 (2006).
[11] P. A. Casey and P. W. Anderson, Phys. Rev. Lett. **106**, 097002 (2011).
[12] S. c. v. Bogdanovich and D. Popović, Phys. Rev. Lett. **88**, 236401 (2002).
[13] J. Jaroszyński, D. Popović, and T. M. Klapwijk, Phys. Rev. Lett. **89**, 276401 (2002).
[14] S. V. Kravchenko and M. P. Sarachik, Reports on Progress in Physics **67**, 1 (2004).
[15] L. Arrachea, D. Dalidovich, V. Dobrosavljević, and M. J. Rozenberg, Phys. Rev. B **69**, 064419 (2004).
[16] D. Dalidovich and V. Dobrosavljević, Phys. Rev. B **66**, 081107 (2002).
[17] S. Sachdev and N. Read, J. Phys.: Condens. Matter **8**,

9723 (1996).
[18] E. Miranda and V. Dobrosavljević, Reports on Progress in Physics **68**, 2337 (2005).
[19] X. Deng, J. Mravlje, R. Žitko, M. Ferrero, G. Kotliar, and A. Georges, Phys. Rev. Lett. **110**, 086401 (2013).
[20] Y. Imry, *Introduction to Mesoscopic Physics* (Oxford University Press on Demand, 2002).
[21] V. Dobrosavljević, N. Trivedi, and J. M. Valles Jr, eds., *Conductor Insulator Quantum Phase Transitions* (Oxford University Press, 2012).
[22] Y. Song, R. Wortis, and W. A. Atkinson, Phys. Rev. B **77**, 054202 (2008).
[23] D. Semmler, K. Byczuk, and W. Hofstetter, Phys. Rev. B **81**, 115111 (2010).
[24] D. Tanasković, V. Dobrosavljević, E. Abrahams, and G. Kotliar, Phys. Rev. Lett. **91**, 066603 (2003).
[25] M. C. O. Aguiar, V. Dobrosavljević, E. Abrahams, and G. Kotliar, Physica B: Condensed Matter **403**, 1417 (2008).
[26] K. Byczuk, W. Hofstetter, and D. Vollhardt, Phys. Rev. Lett. **102**, 146403 (2009).
[27] Y. Otsuka and Y. Hatsugai, J. Phys.: Condens. Matter **12**, 9317 (2000).
[28] B. Srinivasan, G. Benenti, and D. L. Shepelyansky, Phys. Rev. B **67**, 205112 (2003).
[29] P. B. Chakraborty, P. J. H. Denteneer, and R. T. Scalettar, Phys. Rev. B **75**, 125117 (2007).
[30] R. Kotlyar and S. Das Sarma, Phys. Rev. Lett. **86**, 2388 (2001).
[31] D. Heidarian and N. Trivedi, Phys. Rev. Lett. **93**, 129901 (2004).
[32] H. Bragança, M. C. O. Aguiar, J. Vučičević, D. Tanasković, and V. Dobrosavljević, Phys. Rev. B **92**, 125143 (2015).
[33] C. E. Ekuma, S.-X. Yang, H. Terletska, K.-M. Tam, N. S. Vidhyadhiraja, J. Moreno, and M. Jarrell, Phys. Rev. B **92**, 201114 (2015).
[34] S. V. Kravchenko, W. E. Mason, G. E. Bowker, J. E. Furneaux, V. M. Pudalov, and M. D'Iorio, Phys. Rev. B **51**, 7038 (1995).
[35] D. D. Sarma *et al.*, Phys. Rev. Lett. **80**, 4004 (1998).
[36] S. Nakatsuji, V. Dobrosavljević, D. Tanasković, M. Minakata, H. Fukazawa, and Y. Maeno, Phys. Rev. Lett. **93**, 146401 (2004).
[37] L. Sanchez-Palencia and M. Lewenstein, Nature Physics **6**, 87 (2010).
[38] While our many-body techniques capture order-parameter fluctuations, they do not include spin-flip processes characteristics of Kondo screening effects of local moments, *e.g.* E. Miranda *et al.*, Phys. Rev. Lett. **78**, 290 (1997) and S. Sen *et al.*, Phys. Rev. B **94**, 235104 (2016). Thus our effort is complementary to other previous calculations.
[39] This section of the *Supplementary Material* discusses our method [55], its numerical implementation and parallelization [56, 57], its applications to various many body problems [58–64] and comparisons with determinantal quantum Monte Carlo results [65, 66].
[40] Our 2D magnetic T_N correspond to correlation length $\xi(T_N) \approx (L)$ (the system size). There is no T_N in 2D with $O(3)$ auxiliary field in $L \to \infty$.
[41] The slight upturn in T_N at small V/t is compatible with the discussion in M. Ulmke, *et. al.* Phys. Rev. B **51** 10411 (1995).
[42] This section of the *Supplementary Material* also includes details of our optical conductivity calculations based on Kubo-Greenwood formalism [67] and its previous benchmarks [68].
[43] D. Heidarian, *Metal-Insulator Transitions In Two Dimensions*, Ph.D. thesis, School of Natural Sciences Tata Institute of Fundamental Research Mumbai (2006).
[44] Since our calculation is on finite system and the lowest temperature accessed is $T = 0.005t$, the expected divergence in $\rho(T)$ as $T \to 0$ for the CA-I is not captured. Thus the optical conductivity data is the best indicator of metal vs insulator.
[45] T. Paiva, Y. L. Loh, M. Randeria, R. T. Scalettar, and N. Trivedi, Phys. Rev. Lett. **107**, 086401 (2011).
[46] There is a also a variation in α with V for a fixed U, details will be reported elsewhere as this is not the central issue being addressed here.
[47] In the absence of quantum ($t = 0$) and thermal ($T = 0$) fluctuations, the line $U = V$ is special, separating a phase with *all* sites singly occupied from another phase with a mixture of occupancies. This is why our metallic phase is close to $U = V$.
[48] Resistivity minimum occurs for all the cases but is pushed to lower temperatures for smaller U, so the fitting is done in the regime where $d\rho/dT > 0$ going up to $T/t = 1$.
[49] Extensions of the present work may include other forms of disorder (hoppings, etc.) as explored in literature [69, 70].
[50] S. Kumar and P. Majumdar, Phys. Rev. Lett. **94**, 136601 (2005).
[51] S. Blawid, A. Deppeler, and A. J. Millis, Phys. Rev. B **67**, 165105 (2003).
[52] E. C. Andrade, E. Miranda, and V. Dobrosavljević, Phys. Rev. Lett. **102**, 206403 (2009).
[53] M. Milovanović, S. Sachdev, and R. N. Bhatt, Phys. Rev. Lett. **63**, 82 (1989).
[54] E. Miranda and V. Dobrosavljević, Phys. Rev. Lett. **86**, 264 (2001).
[55] A. Mukherjee, N. D. Patel, S. Dong, S. Johnston, A. Moreo, and E. Dagotto, Phys. Rev. B **90**, 205133 (2014).
[56] S. Kumar and P. Majumdar, Eur. Phys. J. B **50**, 571 (2006).
[57] A. Mukherjee, N. D. Patel, C. Bishop, and E. Dagotto, Phys. Rev. E **91**, 063303 (2015).
[58] R. Tiwari and P. Majumdar, EPL (Europhysics Letters) **108**, 27007 (2014).
[59] N. Swain, R. Tiwari, and P. Majumdar, Phys. Rev. B **94**, 155119 (2016).
[60] M. Karmakar and P. Majumdar, Phys. Rev. A **93**, 053609 (2016).
[61] S. Tarat and P. Majumdar, Eur. Phys. J. B **88**, 68 (2015).
[62] M. Karmakar and P. Majumdar, Eur. Phys. J. D **70**, 220 (2016).
[63] A. Mukherjee, N. D. Patel, A. Moreo, and E. Dagotto, Phys. Rev. B **93**, 085144 (2016).
[64] N. Swain and P. Majumdar, arXiv:1610.00695 (2016).
[65] R. Staudt, M. Dzierzawa, and A. Muramatsu, Eur. Phys. J. B **17**, 411 (2000).
[66] T. Paiva, R. T. Scalettar, C. Huscroft, and A. K. McMahan, Phys. Rev. B **63**, 125116 (2001).
[67] G. D. Mahan, *Quantum Many Particle Physics* (Plenum Press, New York, 1990).
[68] S. Kumar and P. Majumdar, Eur. Phys. J. B **46**, 237

(2005).
[69] P. J. H. Denteneer, R. T. Scalettar, and N. Trivedi, Phys. Rev. Lett. **87**, 146401 (2001).
[70] P. J. H. Denteneer and R. T. Scalettar, Phys. Rev. Lett. **90**, 246401 (2003).